Scaling Studies for an Actively Controlled Curvature Robotic Pectoral Fin

Jason D. Geder[1], Ravi Ramamurti[1], John Palmisano[2],
Marius Pruessner[3], Banahalli Ratna[3] and William C. Sandberg[4]

[1] Naval Research Laboratory, Laboratory for Computational Physics and Fluid Dynamics, 4555 Overlook Ave SW, Washington, DC 20375
[2] NOVA Research, Inc., Naval Research Laboratory Contractor, 4555 Overlook Ave SW, Washington, DC 20375
[3] Naval Research Laboratory, Center for Bio-molecular Science and Engineering, 4555 Overlook Ave SW, Washington, DC 20375
[4] Science Applications International Corporation, Modeling and Analysis Division, 1710 SAIC Dr, McLean, VA 22102

Abstract. Scaling studies for an actively controlled curvature robotic pectoral fin are presented in detail. Design, development, and analysis of the fin are conducted using a combination of computational fluid dynamics tools and experimental tests. Results include a Generation 2 (Gen2) fin design with approximately 3x more surface area and a slightly larger aspect ratio compared with our Generation 1 (Gen1) version. The Gen2 fin demonstrates 9x more thrust production than the Gen1 fin, validating the computational studies. Additionally, changes to the structural design of the ribs and actuation of the rib angles leads to a power savings and a more efficient fin.

Keywords: bio-inspired, pectoral fin, active curvature control, UUV, station-keeping

1 Introduction

Despite the broad range of missions enabled by traditional propeller-driven underwater vehicles, there still exists a maneuverability gap between what these current systems offer and what is needed in many dynamic near-shore environments. In these regions where precise positioning and small radius maneuvers are required, fish have demonstrated the agility needed to effectively operate. As such, researchers have studied the fin mechanisms of various fish species [1][2]. Within fish swimming, articulation of the pectoral fins has been shown to produce forces and moments ideal for high-maneuverability in low-speed and hovering operations [3]. Several investigators have developed and adapted passively deforming robotic pectoral fins onto unmanned underwater vehicles (UUVs) [4][5][6][7], whereas others have pursued the development of active control deformation pectoral fins [8][9][10][11].

To enable unmanned vehicle missions in near-shore underwater environments, we have studied the swimming mechanisms of a particular coral reef fish, the Bird wrasse

(*Gomphosus varius*). Inspired by the pectoral fin of this species, we have designed a robotic fin based on computational fluid dynamics (CFD) studies of the forces and moments generated by the flapping fins [9]. The resulting robotic fin uses active curvature control through actuation of individual ribs to produce desired propulsive forces [12].

Results of implementation and testing of this Generation 1 (Gen1) robotic fin on an unmanned vehicle platform have demonstrated the capabilities of the fin [13], and have also validated our computational models [9]. However, this original vehicle design lacked additional mission-enabling payload space, and the force production capability of the fins was insufficient for operations in targeted near-shore environments. To facilitate an upgrade to a vehicle capable of precise maneuvering and station-keeping in complex near-shore environments such as in harbors and around piers, we investigate issues in fin scaling as well as necessary changes to fin construction and actuation.

Initial fin redesign was driven by CFD analysis of thrust production as well as structural consideration for selection and placement of actuators. The most important factors in this redesign are fin area and aspect ratio, fin rib rigidity, and actuator performance. Based on the CFD results and actuator performance studies, a Generation 2 (Gen2) fin is built and experimental tests are conducted to demonstrate thrust production improvement over the Gen1 fin and to validate our CFD tool for studying fin geometry changes.

2 Scaling Motivation

In developing a UUV for a general class of operations, one design constraint is that the vehicle must have the propulsion and control authority to achieve desired maneuvering performance. The NRL Pectoral Fin UUV (PFUUV) is intended for low-speed operations in near-shore environments where station-keeping and precise positioning are essential performance criteria. The vehicle must be able to hold position in the presence of wave and current flow disturbances in areas such as harbors and shallow channels. Looking at flow velocity data from various potential operating locations, the PFUUV should be able to counter flows of up to 2.0 knots (1.0 m/s) [14][15]. The Gen1 vehicle demonstrated a top speed performance of 0.8 knots (0.4 m/s), indicating a need to scale up the fin design for improved thrust capability.

In addition to fin thrust, the second major design constraint is vehicle payload capacity. While the Gen1 vehicle has onboard space limited to electronics for basic vehicle operation, a mission capable vehicle requires additional space for payloads such as sonar, a ballast system, and modular mission-specific equipment. Discussion of the UUV sizing and payload requirements are beyond the scope of this paper, but a Gen2 vehicle hull design has been selected (Figure 1) and drag characteristics are modeled for fin scaling studies.

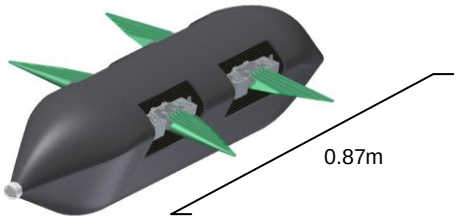

Fig. 1. Gen2 vehicle hull design with four-fin actuation. CFD was used to design for low drag based on volumetric constraints.

2 Computational Studies of Fin Scaling

Computational studies were performed to investigate changes to the fin in both spanwise rib rigidity and fin surface area. To limit our parameter search, we constrained the fin flapping frequency, f, and stroke amplitude, Φ_B, to values achieved in the Gen1 fin [13]. The computational results provided the basis for the Gen2 fin design.

2.1 Spanwise Rib Rigidity

The Gen1 fin was designed with individual, spanwise-directed ribs that are deflected using a push-pull actuation at the rib base [9]. However, finite element stress analysis determined as the fin length scales up linearly, rib base actuator torque must increase exponentially to retain desired curvature. For a fin twice the length of the Gen1 fin, and factoring in compliant structure design modifications of the ribs, the push-pull actuating servos would require 6x the torque of the Gen1 rib servos. This would necessitate much larger motors, and also presented a large efficiency loss. To aid in a redesign that would mitigate this size and power burden, a study of spanwise rib flexibility was conducted. It has been determined that chordwise, or leading edge to trailing edge direction, curvature in the fin is needed to produce the force-time histories for desired thrust generation [16]. However, the effect of spanwise, or fin root to fin tip direction, curvature on thrust generation was not previously studied.

The computational results of a comparison of fin gaits, identical in all respects except rib rigidity, show that spanwise curvature of the ribs does have an effect on fin thrust production for a set of kinematics designed to produce forward thrust. Figure 2 shows thrust comparison for two fins of equal surface shape, surface area, stroke amplitude, stroke frequency, and rib tip deflection. The only difference in fin motion is the curvature of the ribs from base to tip. For this set of fin kinematics, the fin with spanwise rigid ribs actually demonstrates a thrust benefit over the fin with spanwise flexible ribs. The change from spanwise flexible to spanwise rigid ribs results in more fluid being displaced in the chordwise direction than in a spanwise direction, which in turn generates the higher peak thrust seen during the midstroke.

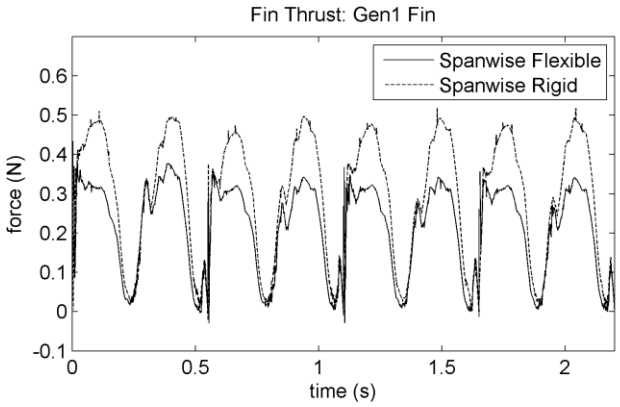

Fig. 2. Gen1 fin thrust-time histories for a fin with stroke frequency f = 1.8 Hz and Φ_B = 85 degrees.

2.2 Fin Surface Area

Computational studies of both drag on the notional Gen2 vehicle hull and thrust from scaled fin models are performed to determine the Gen2 fin design that will enable the required vehicle performance of 1 m/s forward speed (or holding position in a 1 m/s flow).

Gen2 vehicle drag at 1 m/s was computed as 0.3 N (Figure 4) for a smooth hull. However, up to 4 N of drag occurs at this same speed if the portholes where the fins are anchored are completely open to the flow due to large stagnation points inside the portholes. Practical construction of the Gen2 vehicle will not allow for completely solid, closed portholes, but mechanical designs are being investigated to negate this issue.

Based on Gen1 fin thrust results, we scaled the fin surface area using Equation 1 where F_T is the fin generated thrust, ρ is fluid density, V_{tip} is the instantaneous tip velocity of the fin leading edge, A_{fin} is the fin area, and C_T is the coefficient of thrust. Researchers have studied the effects of Reynold's number (*Re*) and Strouhal number (*St*) on the thrust coefficient of flapping mechanisms [17][18]. They have found that for a forward thrust producing kinematics set, the effect of *Re* is minimal in the range considered, and that forces collapse for the same *St*. Further, we have found in past research that for a flapping fin at zero freestream flow (U_∞ = 0), the thrust coefficient is constant for a given set of rib kinematics, and fin thrust scales proportional to fin surface area and to the square of fin tip velocity [19].

$$F_T = \tfrac{1}{2}\rho {V_{tip}}^2 A_{fin} C_T \ . \qquad \textbf{(1)}$$

Using Equation 1, the Gen2 fin geometry was scaled up in span length from 0.10 m to 0.18 m, and in chord length from 0.060 m to 0.095 m. The width of the ribs at the base is also increased, and these changes correspond to a 3x increase in fin area

and a 1.8x increase in fin tip speed. This leads to an estimated fin thrust increase for the Gen2 fin of 9.2x over the Gen1 fin. Computational results yield an 8.4x increase, and this difference from the analytical results is seen in Figure 3 which shows the computational force-time history of the Gen2 fin results compared with the Gen1 fin results scaled by area and tip speed. The Gen1 fin benefited from a thrust peak just after stroke reversal due to a wake capture effect that the Gen2 fin does not experience.

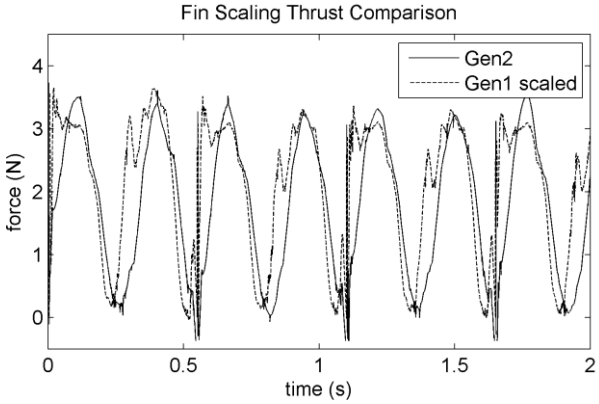

Fig. 3. Gen2 fin thrust-time history compared with scaled thrust-time history of Gen1 fin (scaled by 3.0x fin area and 1.8x fin tip velocity). Results are presented for a fin at $U_\infty = 0$ with $f = 1.8$ Hz, $\Phi_B = 85$ degrees.

The fin thrust for four fins ($f = 1.8$ Hz, $\Phi_B = 85$ degrees) at various flow speeds is shown in Figure 4 along with the computed hull drag. These results indicate that the Gen2 vehicle will reach a maximum speed, where thrust forces equal drag forces, of 0.9 m/s (1.8 knots) with open fin portholes. However, even modest reduction in vehicle drag by partially closing the portholes will allow for the desired two knot vehicle speeds (Figure 4).

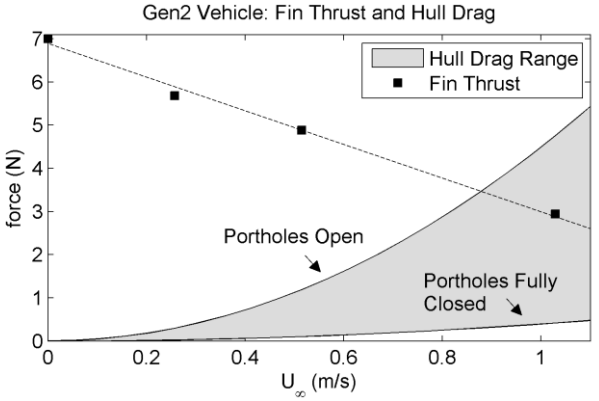

Fig. 4. Gen2 four-fin thrust for $f = 1.8$ Hz and $\Phi_B = 85$ degrees, compared with Gen2 vehicle hull drag.

3 Fin Redesign and Construction

Using the results of the computational analysis, a Gen2 mechanical fin was designed to match the fin stroke and rib deflection frequencies and amplitudes of the Gen1 fin. Improvements in structural and materials robustness were also desired.

3.1 Actuator Selection

An actuator selection process for the Gen2 fin identified two servos, one for fin bulk rotation and one for individual rib rotation, capable of matching the frequency response characteristics of the Gen1 fin (Figure 5).

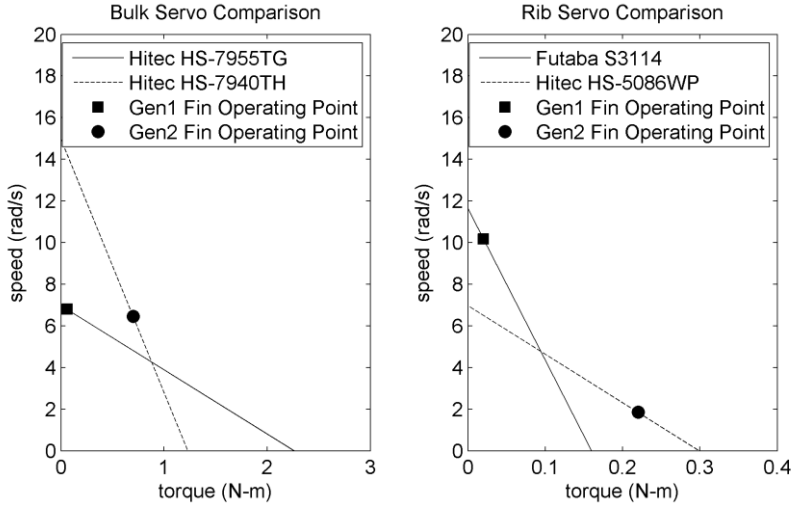

Fig. 5. Average rotational speed comparison of the Gen1 and Gen2 fins and ribs based on servo specifications and fin applied torque.

The Gen1 fin stroke bulk rotation is driven by a Hitec HS-7955TG servo and the speed-torque curve for this actuator shows that at 0.06 N-m torque (the maximum torque on the servo in experimental testing) the servo shaft rotates at 6.7 rad/s. It is important that this speed can be matched by the Gen2 fin stroke for the scaling results of the computational studies to be valid as stroke frequency and amplitude were assumed to be the same. At the 0.75 N-m of maximum torque anticipated on the Gen2 bulk stroke axis, the Hitec HS-7940TH servo is capable of 6.5 rad/s speed. This will provide the Gen2 fin with a similar stroke frequency and amplitude response to the Gen1 fin.

The Gen2 individual rib servo chosen, the Hitec HS-5086WP, has a slower anticipated shaft speed than the Futaba S3114 provided on the Gen1 fin ribs, but the 1.8 rad/s speed at maximum torque of 0.24 N-m is enough to achieve the desired 15-20 degree rib deflection changes during the fin stroke. Additionally, the Hitec HS-5086WP consists of a waterproof design that will reduce failures during operation.

3.2 Fin Ribs and Skin

As computational results show fin thrust is not negatively affected by more spanwise-rigid ribs, the Gen2 fin ribs have been designed for direct actuation of rotation angle. This is different from the push-pull mechanism of the Gen1 ribs (Figure 6). This direct actuation allows for 20% greater rib tip deflection for equal servo axis rotation, significantly reduces the torque required to hold the rib in place, and eliminates the concerns commonly associated with material fatigue.

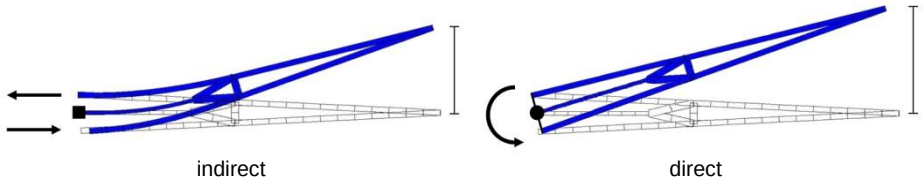

Fig. 6. Indirect push-pull actuation of a fin rib compared with direct actuation of a fin rib. The indirect actuation puts more stress on fragile points near the base of the rib, and also requires more torque to move the rib and hold in position.

4 Experimental Results

Our initial set of experiments on the Gen2 fin focused on forward thrust production from a set of fin kinematics defined as the forward gait [9]. While an exact comparison cannot be made between the Gen1 and Gen2 fins due to changed rib structure and different servo characteristics, our results offer experimental evidence on the effects of fin scaling. Our goal for the Gen2 design was not to exactly mimic the fin on a larger scale, but to create a fin that produces enough thrust to propel a vehicle in excess of 2 knots. For the results shown here, the Gen1 and Gen2 fins have matching commanded rib tip deflections and curvature-time histories.

Forward gait experiments were conducted for both fins over a series of stroke frequencies and amplitudes. A six degree-of-freedom force and torque sensor from ATI Industrial Automation (Nano17 IP68) was used to measure the fin forces.

Figure 7 shows fin thrust as function of actual stroke frequency and commanded stroke peak-to-peak amplitude. Maximum average thrust for the Gen2 fin is 1.1 N, and occurs at f = 1.4 Hz and $\Phi_{B,c}$ = 100 degrees (Φ_B = 90 degrees), where $\Phi_{B,c}$ is commanded peak-to-peak stroke amplitude. At the same frequency and rotation for the Gen1 fin, average thrust is 0.13 N. This represents an 8.5x increase in thrust production from Gen1 to Gen2 fin with equal (or very similar) stroke parameters.

While the Gen2 fin produces 8.5x greater thrust than the Gen1 fin, power consumption only increases 23%, from 12.0 W to 13.5 W, demonstrating a 7x improvement in thrust efficiency. These results do not fully indicate if the efficiency savings was gained from changing the rib drive from indirect push-pull actuation to direct angular actuation (Figure 6), fin size scaling, or a combination of these two factors. Further studies would need to be done to determine the specific cause of

increased thrust efficiency. It has, however, been experimentally determined that the servos used in the Gen2 design are 2x more efficient than those in the Gen1 design.

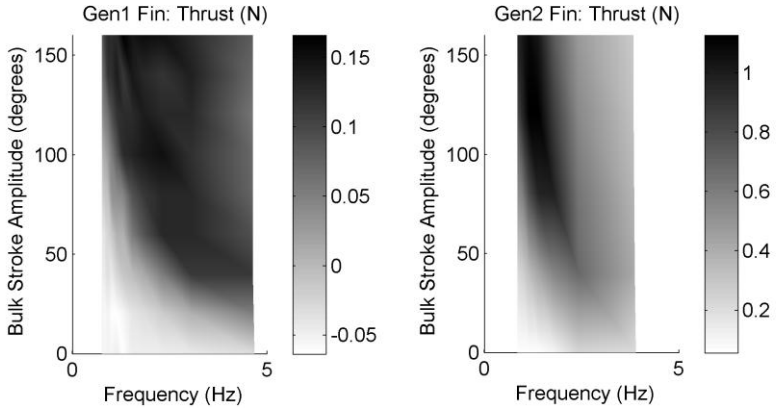

Fig. 7. Gen1 and Gen2 single fin thrust over a range on stroke frequencies and amplitudes.

Figure 8 shows the experimental force-time history of thrust and lift for the Gen1 and Gen2 fins at f = 1.4 Hz and $\Phi_{B,c}$ = 100 degrees. In addition to the 8.5x increase in mean thrust, peak-to-peak thrust increases by 8.0x. Average lift for the forward gait in both the Gen1 and Gen2 fins is zero as the stroke is symmetric about the horizontal plane. Peak-to-peak lift increases by 4.0x.

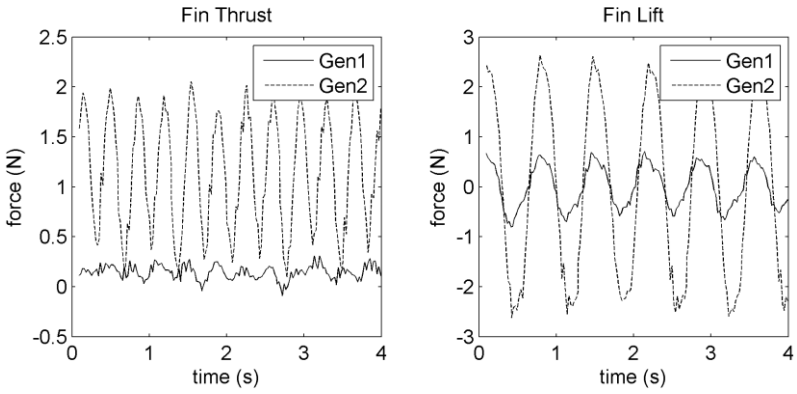

Fig. 8. Gen1 and Gen2 single fin experimental thrust and lift compared for f = 1.4 Hz and $\Phi_{B,c}$ = 100 degrees.

5 Discussion and Conclusions

The experimental work presented in this paper highlights that even though we have not built a perfectly representative scaled version of the Gen1 fin, the results obtained demonstrate the effects of fin scaling. Both computational analyses and the

mechanical design produced a Gen2 fin that generates the desired thrust for our specific mission requirements.

The results in Fig. 7 show not only the stroke frequency and amplitude where maximum average thrust is achieved, but also the full range of fin thrusts at different operating points. One noticeable difference between thrust results of the forward gait for the Gen1 and Gen2 fins is that the Gen1fin has a peak average thrust at a higher flapping frequency than the Gen2 fin. This could indicate a larger envelope of operating points in the frequency-amplitude domain for the Gen1 fin, which in turn points to differences in the fin curvatures caused by a combination of the rigid ribs and to differences in the fin and rib actuators. In nature, we see that as organisms increase in size and weight, the frequency of their flapping decreases [20].

For the forward gait presented in Figure 8, where both the Gen1 and Gen2 fins are actuated at f = 1.4 Hz and $\Phi_{B,c}$ = 100 degrees (Φ_B = 90 degrees for both fins), we can make a comparison of the fin improvement to that seen in the computational studies. The 8.5x increase in experimentally measured thrust from Gen1 to Gen2 fins matches well with the 8.4x increase seen in CFD, and serves to validate our computational models. The experimental and CFD runs have been carried out at slightly different operating conditions (f = 1.4 Hz for experimental, f = 1.8 Hz for computational), but scaling laws apply as shown in previous studies [18].

Also for the case presented in Figure 8, the power consumed by the Gen1 fin is 12.0 W, and the portion of that attributed to the bulk stroke servo is 2.5 W. The power consumed by the Gen2 fin is 13.5 W, 7.0 W of which is for the bulk stroke servo. Predictably, the power consumed by the bulk stroke servo is a greater percentage of the total power in the Gen2 fin than in the Gen1 fin. In fact, the total power consumed by all the individual rib servos decreases from 9.5 W in the Gen1 fin to 6.5 W in the Gen2 fin, even though the servos in the Gen2 fin need to hold position under higher dynamic pressures. This total decrease in rib servo power consumption indicates a combination of reduced mechanical losses in the servos and smaller torque on the servos in the Gen2 fin than the Gen1 fin.

In summary, a fin scaling study was presented which demonstrates the use of computational studies in scaling up an actively controlled curvature robotic pectoral fin for increased thrust production. This study was limited to looking at forward thrust generating kinematics, but experimental analysis validated the computational approach to design. Further, improvements in fin rib design and actuation yielded a Gen2 fin that produced 8.5x more thrust than a Gen1 fin while only increasing power consumption by 23% leading to a fin that is 7x more efficient in thrust production.

Acknowledgments. The authors would like to acknowledge the Naval Research Laboratory and the Office of Naval Research for sponsoring this research.

References

1. Colgate, J.E., Lynch, K.M.: Mechanics and Control of Swimming: A Review. IEEE Journal of Oceanic Engineering, 29, 660--673 (2004).
2. Bandyopadhyay, P.R.: Trends in biorobotic autonomous undersea vehicles. IEEE Journal of Oceanic Engineering, 30, 109--139 (2005).

3. Walker, J., Westneat, M.A.: Labriform propulsion in fishes: kinematics of flapping aquatic flight in the bird wrasse, *Gomphosus varius*. Journal of Experimental Biology, 200, 1549--1569 (1997).
4. Kato, N.: Hydrodynamic Characteristics of a Mechanical Pectoral Fin. ASME Journal of Fluids Engineering, 121, 605--613 (1999).
5. Kato, N.: Control Performance of a Fish Robot with Mechanical Pectoral Fins in the Horizontal Plane. IEEE Journal of Oceanic Engineering, 25, 1, 121--129 (2000).
6. Hobson, B., Murray, M., Pell, C.A.: PilotFish: Maximizing Agility in an Unmanned-Underwater Vehicle. Proceedings of the International Symposium on Unmanned Untethered Submersible Technology, Durham, NH (1999).
7. Licht, S., Polidoro, V., Flores, M., Hover, F.S., Triantafyllou, M.S.: Design and Projected Performance of a Flapping Foil AUV. IEEE Journal of Oceanic Engineering, 29, 3, 786—794 (2004).
8. Ando, Y., Kato, N., Suzuki, H., Ariyoshi, T., Suzumori, K., Kanda, T., Endo, S.: Elastic Pectoral Fin Actuators for Biomimetic Underwater Vehicles. Proceedings of the 16th International Offshore and Polar Engineering Conference, pp. 260--267 (2006).
9. Palmisano, J., Ramamurti, R., Lu, K.J., Cohen, J., Sandberg, W.C., Ratna, B.: Design of a Biomimetic Controlled-Curvature Robotic Pectoral Fin. IEEE Int. Conf. on Robotics and Automation, Rome, Italy (2007).
10. Moored, K.W., Smith, W., Chang, W., Bart-Smith, H.: Investigating the thrust production of a myliobatoid-inspired oscillating wing. 3rd International CIMTEC Conference, Acireale, Italy (2008).
11. Tangorra, J., Davidson, N., Hunter, I., Madden, P., Lauder, G., Dong, H., Bozkurttas, M., Mittal, R.: The Development of a Biologically Inspired Propulsor for Unmanned Underwater Vehicles. IEEE Journal of Oceanic Engineering, 32, 3, 533—550 (2007).
12. Geder, J.D., Ramamurti, R., Palmisano, J., Pruessner, M., Ratna, B., Sandberg, W.C.: Dynamic Performance of a Bio-Inspired UUV: Effects of Fin Gaits and Orientation. Proceedings of the 17th International Symposium on Unmanned Untethered Submersible Technology, Portsmouth, NH (2011).
13. Geder, J.D., Ramamurti, R., Palmisano, J., Pruessner, M., Sandberg, W.C., Ratna, B.: Four-fin Bio-inspired UUV: Modeling and Control Solutions. ASME International Mechanical Engineering Congress and Exposition, International Mechanical Engineering Congress and Exposition, 2011-64005 (2011).
14. National Oceanic and Atmospheric Administration Tides and Currents Information, http://tidesandcurrents.noaa.gov/
15. Clem, T.: Oceanographic Effects on Maritime Threats: Mines and Oil Spills in the Strait of Hormuz. Master's Thesis, Naval Postgraduate School, Monterey, CA (2007).
16. Ramamurti, R., Sandberg, W.C.: Computational Fluid Dynamics Study for Optimization of a Fin Design. Proceedings of the 24th AIAA Applied Aerodynamics Conference, AIAA-2006-3658, San Francisco, CA (2006).
17. Bozkurttas, M., Mittal, R., Dong, H., Lauder, G.V., Madden, P.: Low-dimensional models and performance scaling of a highly deformable fish pectoral fin. Journal of Fluid Mechanics, 631, 311—342 (2009).
18. Ramamurti, R., Sandberg, W.: Simulation of Flow About Flapping Airfoils Using Finite Element Incompressible Flow Solver. AIAA Journal, 39, 2, 253—260 (2002).
19. Ramamurti, R., Geder, J.D., Palmisano, J., Ratna, B., Sandberg, W.C.: Computations of Flapping Flow Propulsion for Unmanned Underwater Vehicle Design. AIAA Journal, 48, 1, 188--201 (2010).
20. Azuma, A.: The Biokinetics of Flying and Swimming. Tokyo: Springer (1992).